Tsuyama et al., https://doi.org/10.1083/jcb.201604065

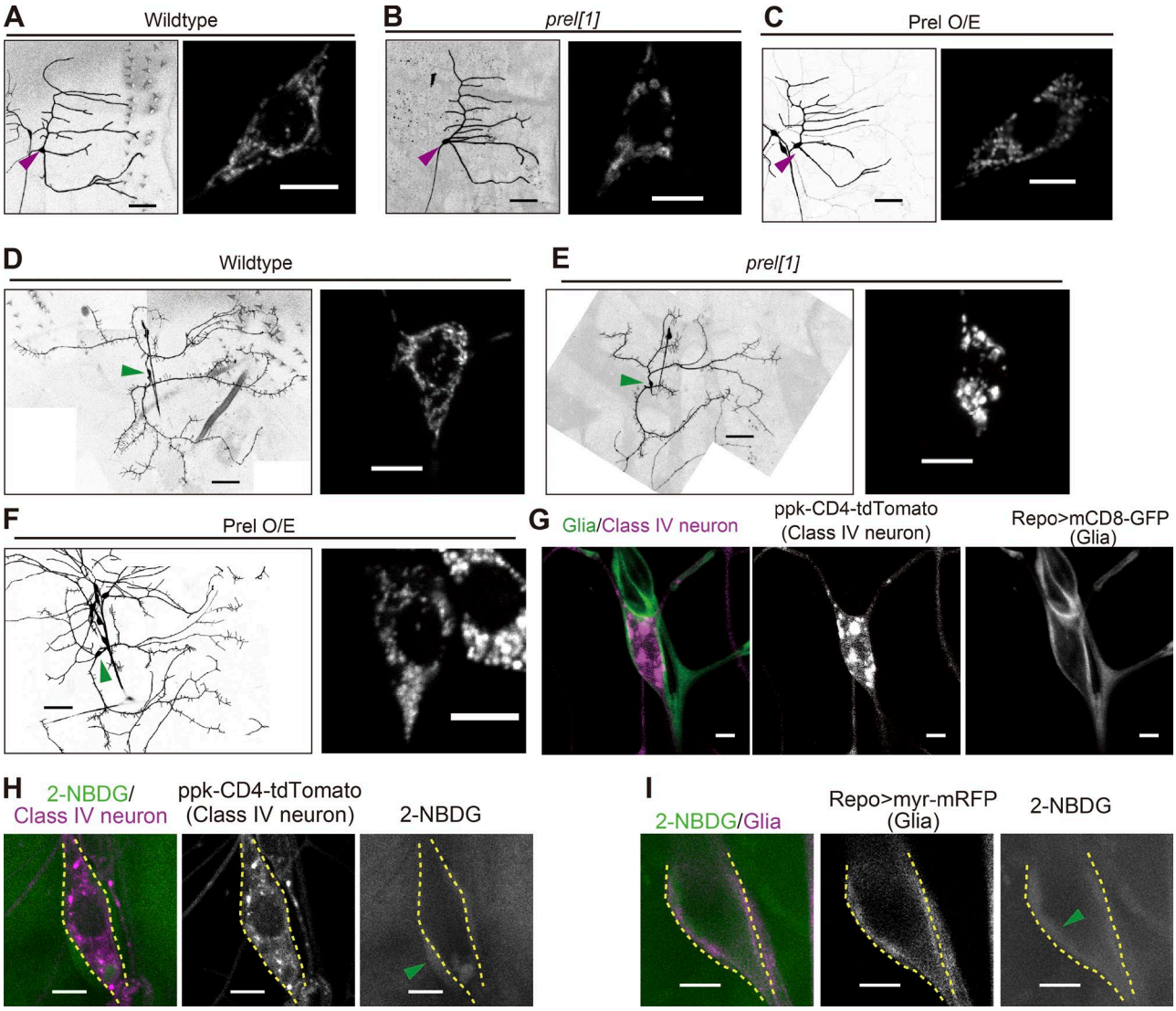

Figure S1. **Mild dendritic losses of class I and III neurons with altered *prel* function and uptake of 2-NBDG by glial cells that wrap around class IV neurons of the control genotype.** Representative dendritic and somal mitochondrial morphologies of wild-type (A and D), *prel[1]* mutant (B and E), and Prel-overexpressing (C and F) neurons of class I (A–C) and III (D–F). Magenta and green arrowheads indicate the cell bodies of class I and III neurons, respectively. Dendritic arbors and mitochondria were visualized with membrane-bound GFP and mito-GFP, respectively. Bars: (dendrite images) 50 µm; (mitochondrial images) 5 µm. (G) Two-color imaging of a class IV neuron (magenta) with *ppk-CD4-tfTomato* and glial cells (green) with *Repo-Gal4* and *UAS-mCD8-GFP*. (H and I) Two-color imaging of 2-NBDG–positive cells (green) and a class IV neuron by *ppk-CD4-tfTomato* (H, magenta) or a glial cell (I, magenta) with *Repo-Gal4* and *UAS-myr-mRFP*. Outlines of the class IV neuron and those of the glia are marked by yellow broken lines in H and I, respectively. The 2-NBDG–positive cell wraps the soma of class IV neuron (H, green arrowhead) and it overlaps the glia (I, green arrowhead). To clearly reveal features, these images were nonlinearly adjusted. See also Fig. 3 D (control). Bars, 5 µm (G–I).

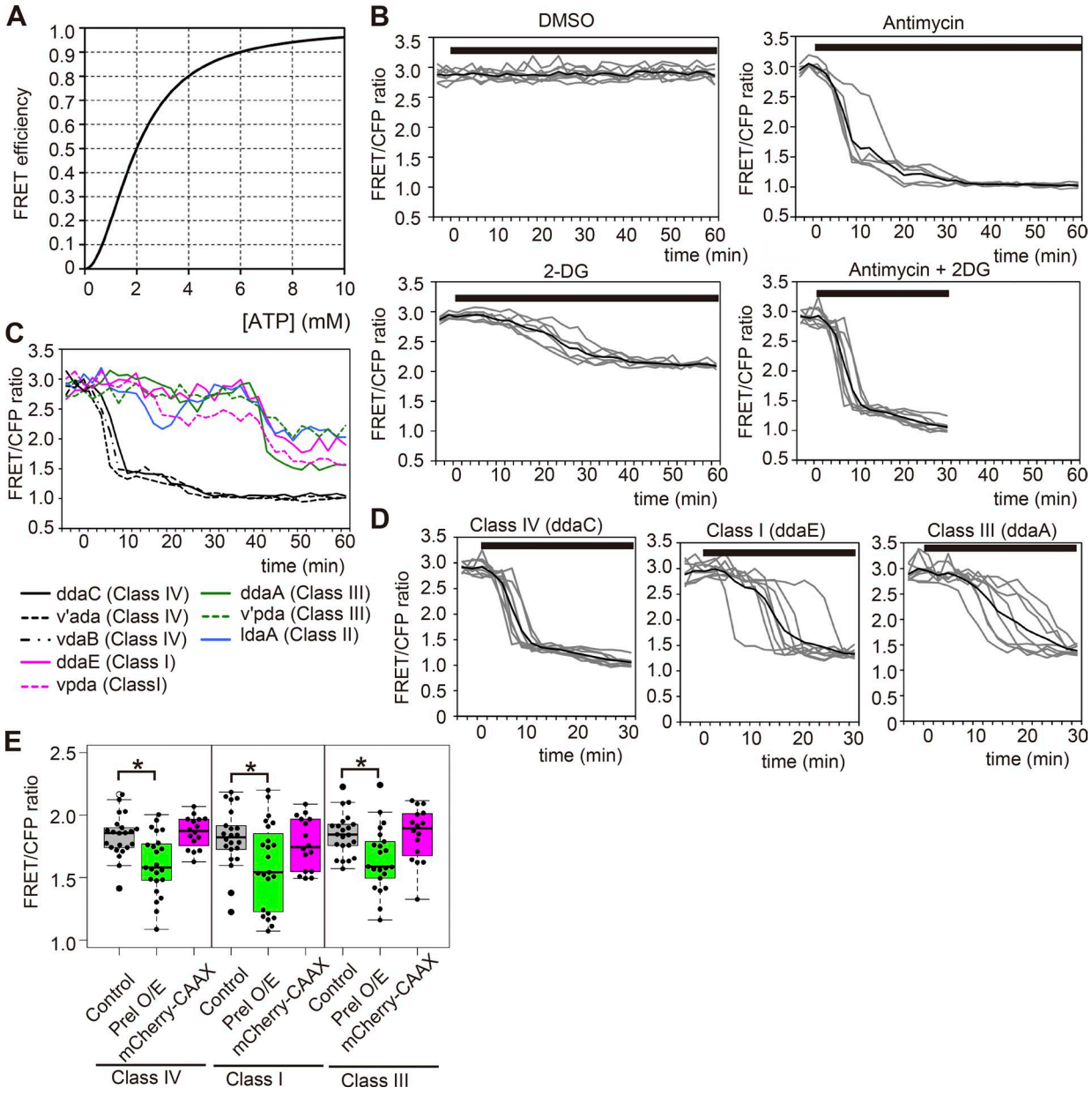

Figure S2. **ATeam1.03NL (AT[NL]), FRET imaging of neurons of the wild-type genotype in the presence of inhibitors of ATP production pathways, and imaging of control or Prel O/E neurons at early L1.** (A) FRET efficiency of AT[NL] as a function of ATP levels calculated by the Hill equation. With the apparent dissociation constant value of ∼2 mM at 25°C and Hill coefficient of ∼2 of the purified AT[NL] probe, the probe is expected to detect changes in ATP levels in the range of 0.5 to 4 mM. (B) Raw data of Fig. 2 C. The effects of inhibitors of ATP-producing pathways on the FRET signals of AT[NL] in individual da neurons. Gray and black lines indicate the signals in individual neurons and the mean signal value in class IV neurons, respectively. (C) The effect of 100 µM AM on the FRET signals of AT[NL] in single da neuron in the same single abdominal hemisegment of a larva. (D) Changes in the FRET signals of AT[NL] in each da neuronal class in the presence of 50 µM AM plus 50 mM 2-DG. In contrast to the rapid decrease in the FRET signal of AT[NL] in class IV neurons treated with AM/2DG, there were lag periods preceding drops of the FRET signals in class I and III neurons. These delays could be explained by several possibilities. One possibility is that ATP levels in class I and III neurons may be too high for AT[NL] to detect initial changes induced by inhibitors. In addition, or alternatively, differences in the effect of inhibitors or differential capacities to buffer ATP reductions between each Class could be a cause of the delayed declines. We could not address this issue further because of technical limitations. (E) The effect of Prel O/E on the FRET signals of AT[NL] in each class at early L1. Similar reductions were found in all subclasses. The data from class IV neurons in Fig. 2 D are shown for comparison. *, $P < 0.05$.

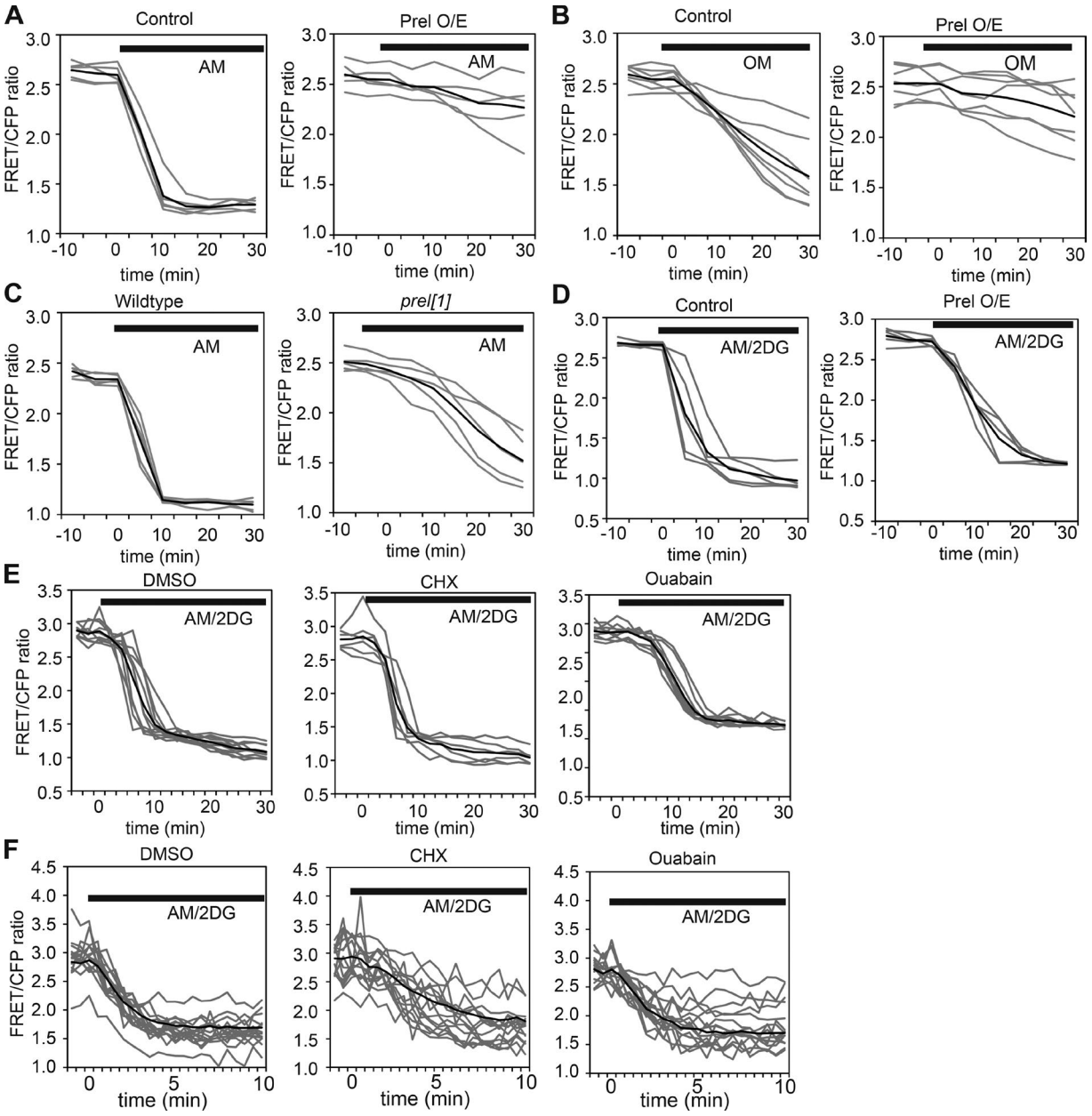

Figure S3. **Responses of individual class IV neurons of O/E or loss of function of *prel* to inhibitors of ATP production pathways.** Gray and black lines indicate the signals in individual neurons and the mean signal values in class IV neurons, respectively. (A and B) Raw data of Fig. 3 B. Oligomycin (OM) is an inhibitor of ATP synthase. (C) Raw data of Fig. 3 C. (D) Raw data of Fig. 3 E. (E) Raw data of Fig. 8 A. (F) Raw data of Fig. 8 B.

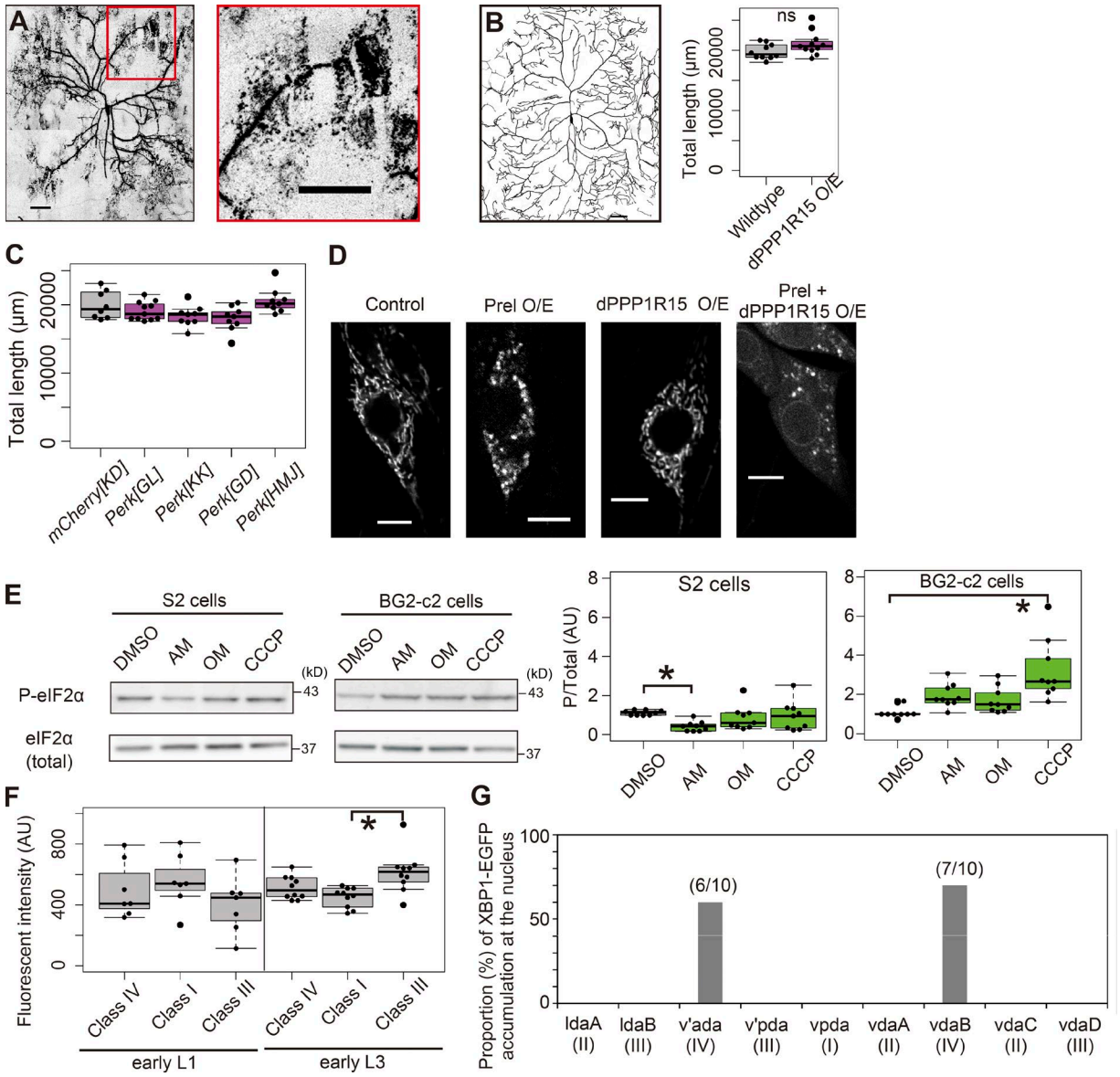

Figure S4. **Genetic interaction between Prel and dPPP1R15, levels of eIF2α phosphorylation in cultured cells in the presence of various mitochondrial inhibitors, and activation of the XBP1 pathway in wild-type neurons.** (A) Representative images of a class IV neuron coexpressing Prel and dPPP1R15 whose dendritic arbors were apparently engulfed by the epidermis (n = 4 in 17 neurons we observed). A red box in the left image is enlarged in the right image. Fluorescent signals of a membrane-bound fluorescent marker for the class IV dendritic arbors (*ppk-CD4-tdGFP*) were detected at the body wall, where the signals were absent in control animals. Hexametric patterns of the incorporated signals were reminiscent of the cellular morphology of the epidermis. This observation is consistent with the finding that the epidermis has phagocytic activity to clear artificially or developmentally severed degenerating class IV dendritic processes (Han et al., 2014). These facts suggest that Prel plus dPPP1R15 coexpression sometimes damages dendritic arbors of class IV neurons, leading to engulfment of part of the arbor by the epidermis, resulting in the severer dendritic loss phenotype (Fig. 4 E, right). (B and C) Promotion of eIF2α dephosphorylation in wild-type class IV neurons does not affect the morphologies of their dendritic arbors. (B) An example of dendritic arbors (left) and quantification of the total dendritic length (right). (C) Quantification of the total dendritic length of *Perk*-KD class IV neurons. A significant change was not detected. ANOVA followed by post-hoc Dunnett's test (versus *mCherry[KD]*). (D) Representative images of mitochondrial morphologies in the cell bodies of Class IV neurons overexpressing Prel, dPPP1R15, or Prel plus dPPP1R15. (E) S2 cells or BG2-c2 cells were treated with 20 nM AM, 40 nM OM, or 15 µM CCCP for 5 h, and levels of eIF2α phosphorylation were examined. Representative immunoblots (left) and quantification of the band intensities of nine biological replicates (right). ANOVA followed by post-hoc Dunnett's test (versus DMSO). *, P < 0.05. (F) *Gal4[21–7]* expression levels in each neuron class. Quantification of fluorescent signals of a *Gal4[21–7]*-driven mCD8::GFP marker. GFP intensity in the cell body was quantified. *, P < 0.05. (G) Quantification of the proportion of wild-type da neurons in lateral and ventral areas of the abdominal hemisegment with XBP1-EGFP accumulation in the nucleus at early L2 (48–52 h AEL). The signals were observed only in class IV neurons (n = 10 for each neuron). Bars: (A) 50 µm; (D) 5 µm. ns, not significant.

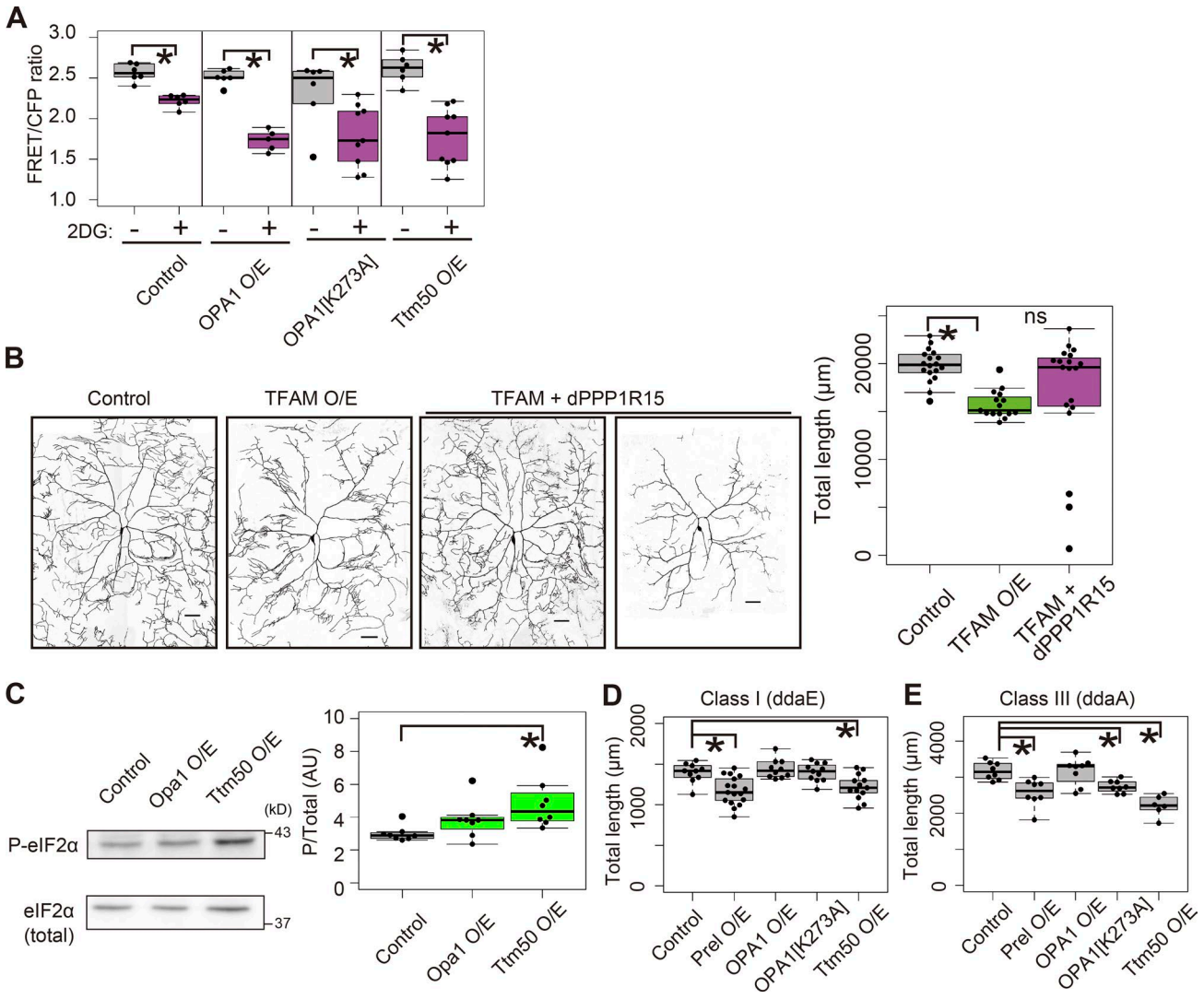

Figure S5. **FRET imaging, levels of eIF2α phosphorylation, and dendrite length of Opa1-, Opa1[K273A]-, or Ttm50-overexpressing da neurons and genetic interaction between TFAM and dPPP1R15.** (A) Quantification of the FRET signals of AT[NL] in class IV neurons expressing Opa1, Opa1[K273A], or Ttm50 in the absence or presence of 50 mM 2-DG, an inhibitor of glycolysis, for 60 min in the fillet preparation. (B) Representative images (left) and quantification (right) of the dendritic arbors of class IV neurons expressing TFAM and TFAM plus dPPP1R15. TFAM O/E reduced the total length and dPPP1R15 coexpression appeared to rescue the dendritic loss, although 3 out of 18 coexpressing neurons exhibited severe dendritic loss, which is reminiscent of the bimodal phenotype of class IV neurons coexpressing Prel plus dPPP1R15 (Fig. 4, C and E). ANOVA followed by post-hoc Turkey's HSD test. (C) The effects of Opa1 or Ttm50 O/E in class IV neurons on eIF2α phosphorylation. Representative immunoblots (left) and quantification of the band intensities of eight biological replicates (right). (D and E) The effect of Opa1, Opa1[K273A], or Ttm50 O/E on the dendritic morphologies of class I and III neurons. Quantification of the total dendritic length of class I (D) and III (E) neurons expressing Opa1, Opa1[K273A], or Ttm50. *, $P < 0.05$; ns, not significant.

Provided online are two Excel tables. Table S1 shows statistical tests used, exact p-values, 95% confidence intervals, and sample sizes in figures and gene expression analysis in da neurons with Gal4 enhancer lines. Table S2 shows genotypes used in each experiment.